OPEN ACCESS

UNIVERSITY OF DUNDEE

University of Dundee

A multifaceted approach to identify non-specific enzyme inhibition

Alturki, Mansour S.; Fuanta, Ngolui Rene; Jarrard, Madison A.; Hobrath, Judith V.; Goodwin, Douglas C.; Rants'o, Thankhoe A.; Calderón, Angela I.

Link to publication in Discovery Research Portal

Accepted Manuscript

A multifaceted approach to identify non-specific enzyme inhibition: Application to *Mycobacterium tuberculosis* shikimate kinase

Mansour S. Alturki, Ngolui Rene Fuanta, Madison A. Jarrard, Judith V. Hobrath, Douglas C. Goodwin, Thankhoe A. Rants'o, Angela I. Calderón

Please cite this article as: Alturki, M.S., Fuanta, N.R., Jarrard, M.A., Hobrath, J.V., Goodwin, D.C., Rants'o, T.A., Calderón, A.I., A multifaceted approach to identify non-specific enzyme inhibition: Application to *Mycobacterium tuberculosis* shikimate kinase, *Bioorganic & Medicinal Chemistry Letters* (2017), doi: https://doi.org/10.1016/j.bmcl.2017.12.002

Leave this area blank for abstract info.

A multifaceted approach to identify non-specific enzyme inhibition: Application to *Mycobacterium tuberculosis* shikimate kinase

Mansour S. Alturki[a,d], Ngolui Rene Fuanta[b], Madison A. Jarrard[a], Judith V. Hobrath[c], Douglas C. Goodwin[b], Thankhoe A. Rants'o[a], Angela I. Calderón[a,*]
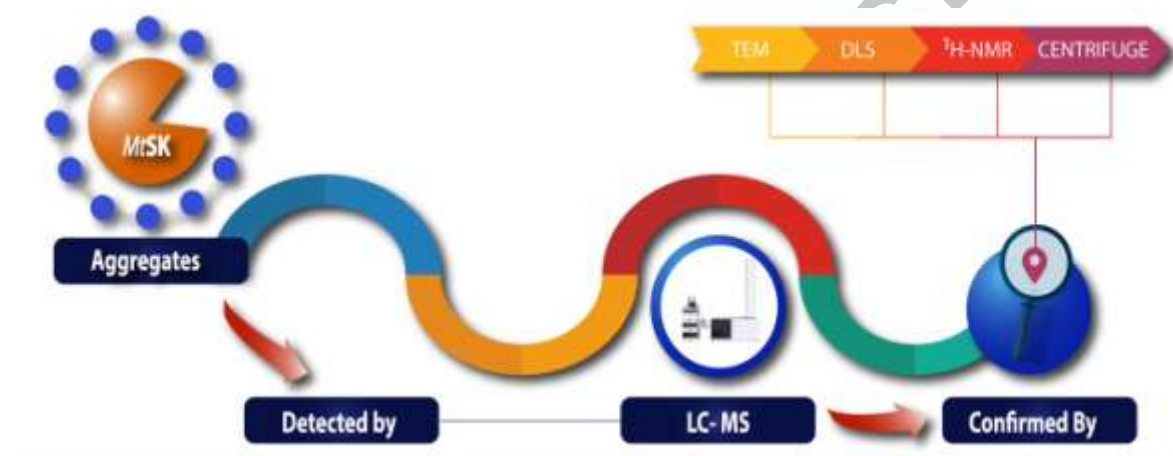
A multifaceted approach to identify non-specific enzyme inhibition: Application to *Mycobacterium tuberculosis* shikimate kinase

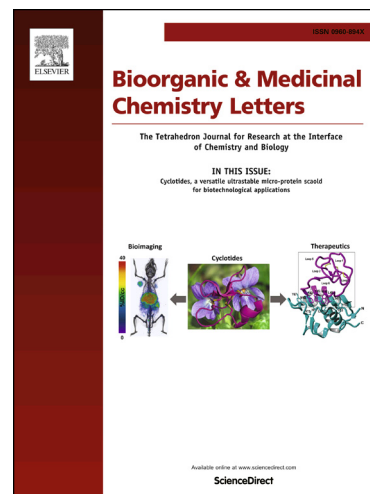Mansour S. Alturki[a,d], Ngolui Rene Fuanta[b], Madison A. Jarrard[a], Judith V. Hobrath[c], Douglas C. Goodwin[b], Thankhoe A. Rants'o[a], Angela I. Calderón[a,*]

[a]*Department of Drug Discovery and Development, Harrison School of Pharmacy, 4306 Walker Building, Auburn University, Auburn, AL 36849, USA.*

[b]*Department of Chemistry and Biochemistry, College of Sciences and Mathematics, 179 Chemistry Building, Auburn University, Auburn, AL 36849, USA*

[c]*Drug Discovery Unit, College of Life Sciences, University of Dundee, Dundee DD1 5EH, United Kingdom*

[d]*Department of Pharmaceutical Chemistry, College of Clinical Pharmacy, Imam Abdulrahman Bin Faisal University, Dammam 34212, Saudi Arabia*

ARTICLE INFO

ABSTRACT

Single dose high-throughput screening (HTS) followed by dose-response evaluations is a common strategy for the identification of initial hits for further development. Early identification and exclusion of false positives is a cost-saving and essential step in early drug discovery. One of the mechanisms of false positive compounds is the formation of aggregates in assays. This study evaluates the mechanism(s) of inhibition of a set of 14 compounds identified previously as actives in *Mycobacterium tuberculosis* (*Mt*) cell culture screening and *in vitro* actives in *Mt* shikimate kinase (*Mt*SK) assay. Aggregation of hit compounds was characterized using multiple experimental methods, LC-MS, ^{1}H-NMR, dynamic light scattering (DLS), transmission electron microscopy (TEM), and visual inspection after centrifugation for orthogonal confirmation. Our results suggest that the investigated compounds containing oxadiazole-amide and aminobenzothiazole moieties are false positive hits and non-specific inhibitors of *Mt*SK through aggregate formation.
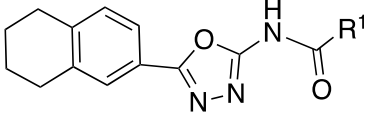
Small molecule aggregators form aggregates or colloids at micromolar concentrations in buffered solutions.[1] Aggregators are commonly found and widely distributed within large compound libraries.[2] These compounds are frequently identified as inhibitors, and they are often prevalent early in drug discovery campaigns.[3] Such compounds may be problematic to identify as false positive because the mechanism by which they inhibit target proteins and enzymes is nonspecific, producing results similar to true positives in a variety of assays.[4]

There are hallmarks for aggregator-based inhibition. Aggregators often show non-competitive inhibition,[5] as well as slowly reversible,[6] and time-dependent inhibition.[7] Of course, true positives can also show these characteristics. However, more particular to aggregators, inhibitor potency as indicated by the kinetic parameters of inhibition, often varies with enzyme concentration.[7] Detergents often reduce or even eliminate inhibition by aggregate-forming false positives.[8] In addition, these compounds are non-specific,[9] inhibiting multiple unrelated enzymes,[10-12] and they show dose-response curves with high Hill slopes.[13] Structure-activity relationships (SAR) may be ambiguous.[14] Finally, particles of varying sizes may be detected in aqueous solutions containing these compounds.[15,16]

Fourteen compounds containing oxadiazole-amide (Table 1) and aminobenzothiazole scaffolds (Table 2) were evaluated in this study. These compounds originated from a library of 404 compounds selected through the Tuberculosis Antimicrobial Acquisition and Coordinating Facility (TAACF) Program of the National Institute of Allergy and Infectious Diseases (NIAID). This set of 404 compounds were in *M. tuberculosis* H37Rv screens performed at Southern Research Institute (SRI).[17-19] The collection was further tested *in vitro* against *M. tuberculosis* shikimate kinase (*Mt*SK). Out of 404 compounds 14 hits displayed >90 % inhibition at concentrations below 50 μM.[20]
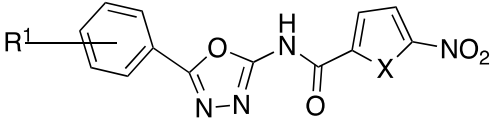
In this study, we investigated aggregate forming properties of compounds in the 14 *Mt*SK hit set, utilizing ESI-LC-MS, proton nuclear magnetic resonance spectroscopy (^{1}H-NMR), dynamic light scattering (DLS), transmission electronic microscopy (TEM). Centrifugation assays were utilized to detect precipitate formation and qualitatively determine the solubility of compounds. The tendency of these compounds to form aggregates was predicted computationally, using the aggregate advisor tool and MycPermCheck software. We have used two controls. The *Mt*SK-specific inhibitor, 3-methoxy-4-{[2-({2-methoxy-4-[(4-oxo-2-thioxo-1,3thiazolidin5ylidene)methyl]phenoxy}methyl)benzyl]oxy}ben-zaldehyde (Fig. S1) was utilized in all experiments except ^{1}H-NMR. Riluzole, a non-aggregator (Fig. S3), was used in ^{1}H-NMR assays.

Table 1. Oxadiazole-amide analogs (1-10)

1-3

Compound	R^1	R^2	R^3
1	n-butyl		
2	Ph-thio-Ethyl		
3	Ph-CH=CH		
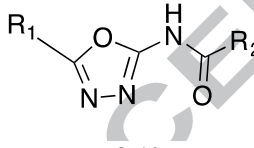
4-5

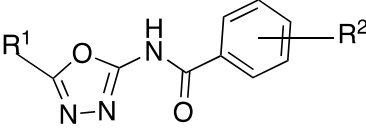| Compound	R^1	R^2	R^3
4	2,4-diMe, X=O		
5	2,5-diMe, X=S		

6-7
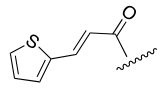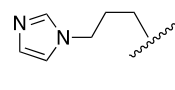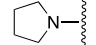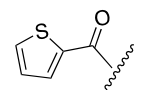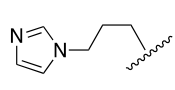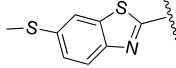
Compound	R^1	R^2	R^3
6	2,4 diMe-Ph	2-Cl	
7	2-Cl-Ph	3-O-Ph	

8-10

Compound	R^1	R^2	R^3
8	4-Br-Ph	t-bu	
9	2-furanyl	4-EtS-Ph	
10	2,4-diMe-Ph	Ph-O-Ethyl	

Table 2. 2-Aminobenzothiazole analogs (11-14)

11-14
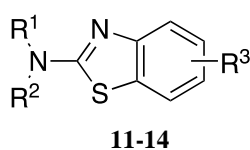
Compound	R^1	R^2	R^3
11			4-Ethyl
12			5,7-dimethyl
13			4,6-difluoro
14		H	6-Acetylamino

Compared to reactions that contained only *Mt*SK and its substrates, inclusion of any one of the compounds resulted in a substantial decrease in S3P production (Table 3) as observed in extracted ion chromatograms (Fig. 1), This indicates inhibition; however, the inhibitory effect was completely eliminated if Triton X-100 was also present or if *Mt*SK concentration in the assays was increased from 0.02 to 0.2 μM. These data indicate that inhibition by these compounds is due, at least in part, to their propensity to form aggregates that non-specifically disrupt *Mt*SK structure. Accordingly, inclusion of Triton X-100 limits formation of aggregates, and therefore, eliminates that contribution to *Mt*SK inhibition. Likewise, inhibition by aggregators is known to be attenuated by an increase in enzyme concentration. Consistent with these findings, inhibition by a known specific inhibitor of *Mt*SK as a control was not eliminated either by the inclusion of detergent or increasing the concentration of *Mt*SK in activity assays. Interestingly, even the control showed potential signs of aggregation, albeit to a much lesser extent than the other compounds. Addition of Triton X-100 increased % inhibition by the control when the concentration of *Mt*SK was 0.2 μM. One explanation is that aggregation was disrupted in the biochemical buffer, permitting the control to behave as a specific inhibitor in the classical sense.
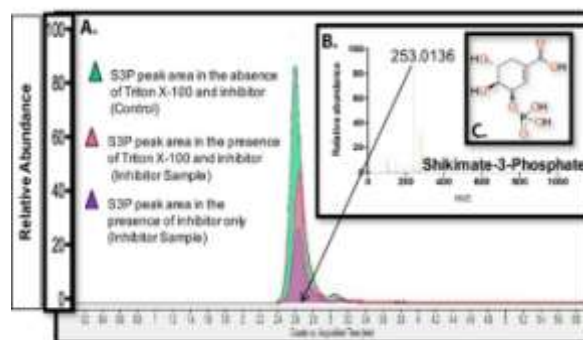
Figure 1. A. An extracted ion chromatogram of shikimate-3-phosphate in different conditions for compound **3**. B. ESI-MS spectrum showing shikimate-3-phosphate (S3P) ionic mass. C. Chemical Structure of shikimate-3-phosphate (S3P).

Table 3. Effect of 0.01% Triton X-100 on *Mt*SK inhibition by oxadiazole-amide and aminobenzothiazole at 100 μM and control at 30 μM.

	0.02 μM *Mt*SK		0.2 μM *Mt*SK	
	Without Triton X-100	With Triton X-100	Without Triton X-100	With Triton X-100
Structure	Inhibition %		Inhibition %	
3	95± 2	0	0	0
4	91.6±0.5	0	0	0
7	90±1	0	0	0
14	97.4± 1	0	0	0
Control	96± 1	98± 1	55± 2	83± 2

With all compounds, a sharp transition to full inhibition occurred over a very narrow range of concentration (Fig. 2) as reflected by Hill coefficients substantially greater than 1. This is a common pattern among non-specific inhibitors.[5] Compounds **3**, **4**, **7**, and **14** incubated with 0.015 μM *Mt*SK showed IC_{50} values of 58.4, 65.72, 38.73, and 60.64 μM, respectively (Table 4). Hill-slope values were 4.7, 8.5, 2.4, 6.1, and 6.7 for compounds **3**, **4**, **7**, **14**, and the control, respectively. Finally, we visually inspected concentration-response curve of compound **3,** reported previously,[20] which showed similar phenomenon to compound **3** in this study. Notably, the control exhibited a similarly steep Hill-slope, this is likely due to the presence of aggregates at higher concentration. The effect of Triton X-100 addition to 0.2 mM *Mt*SK experiments in Table 3 supports this conclusion.
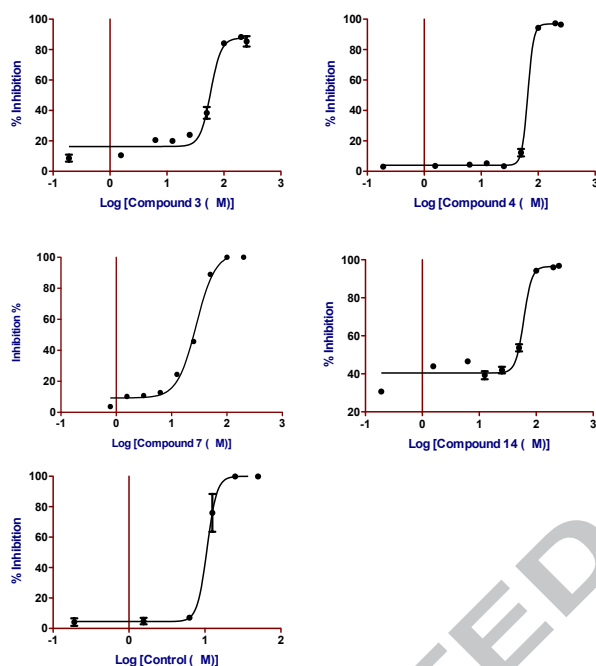

Figure 2. Concentration response-curves values of compounds **3**, **4**, **7**, and **14** and control. All show curve steepness.

Table 4. IC_{50} values of non-specific inhibitors against 0.015 μM purified *Mt*SK.

Compound	IC_{50} (μM) *Mt*SK 0.015 μM
3	58.4 ±0.02
4	65.72 ±0.01
7	38.73 ±0.02
14	60.64 ±0.04
Control	10.10 ±0.02

Table 5 lists computed cLogP (partition coefficient) and LogS (solubility) for the fourteen compounds (Schrödinger software). Computed parameters suggest that compound **11** is the most lipophilic (cLogP 5.148) whereas compound **4** the least hydrophobic (cLogP 1.736). Within this set compound **2** is predicted as least soluble (solubility: -6.854) and compound **9** as most soluble (solubility: -4.246).

Table 5. cLogP and solubility values of test compounds calculated with Schrödinger software package

Structure	cLogP	Solubility*
1	3.637	-5.193
2	4.306	-6.854
3	4.063	-6.247
4	1.736	-4.329
5	2.206	-4.777
6	3.553	-5.466
7	4.446	-6.211
8	2.839	-4.544
9	2.703	-4.246
10	3.728	-5.761
11	5.148	-6.02
12	3.822	-4.688
13	4.262	-5.003
14	3.665	-6.102
Control	5.162	-8.197

With the MycPermCheck tool, Mtb cell wall permeability was predicted for the set of fourteen compounds based on four descriptors listed in Table 6. The predicted permeability was color coded as follows: high permeability scores are colored green (0.82 < score < 1), medium permeability orange (0.55 < score < 0.82) and poor permeability red (score < 0.55). Interestingly, eight compounds were predicted to be highly permeable, namely, **2**, **3**, **6**, **7**, **9**, **11**, **13**, and **14**. These compounds are also associated with higher LogP values within the set. Considering one descriptor only will not guarantee high permeability values. Instead, all descriptors should be taken into consideration. As described by Merget et al.,[21] the computational tool predicts passive diffusion transportation only, which is a limitation of the tool, this suggests that compounds **1**, **4**, **5**, **8**, **10**, and **12** traverse *Mtb* cell wall by other mechanisms. Although the permeability prediction tool is useful for predicting compounds that are expressing their activity through cell wall penetration, absolute confirmation is not expected. Therefore, we suggest that, from the set of 14 compounds, the most active compounds, **4**, **6**, **7**, **8**, **9**, **11**, and **14** (Table 7) should be further investigated so as to understand their mechanism of action.

Table 6. *Mtb* cell wall permeability prediction of oxadiazole-amide and 2-aminobenzothiazole compounds.

Compound number	Score	FOSA	LogP	PISA	accptHB
11	1	201	5.148	415	6.5
7	1	0	4.446	513	5.5
13	0.998	64.3	4.262	352	6.5
3	0.997	209.11	4.063	355	5
2	0.991	253	4.306	329	5.5
6	0.966	160.88	3.553	290	5
9	0.87	131	2.703	313	6
14	0.865	181.64	3.665	263	6.5
10	0.715	301.72	3.728	267	5.75
5	0.152	160.88	2.206	211	6
12	0.118	363.25	3.822	92	2
8	0.136	205.12	2.839	173.3	5
4	0.057	160.89	1.736	221.9	6.5
1	0.024	391.26	3.637	122	5
Control	0.627	229	5.162	309	7.5

FOSA= The hydrophobic part of the solvent accessible surface area (saturated carbon and attached hydrogen atoms), cLogP= Calculated logarithm of compound's partition coefficient between n-octanol and water, PISA= portion of the solvent accessible surface area responsible for π interaction, and accptHB= Number of hydrogen bond acceptors.

Table 7. Anti-*Mtb* phenotypic activity of oxadiazole-amide and 2-aminobenzothiazole

Compound number	TB IC$_{90}$(µg/ml)H37Rv	*Activity level
1	3.04	Medium
2	1.93	Medium
3	1.68	Medium
4	0.69	High
5	3.09	Medium
6	< 0.20	High
7	0.86	High
8	< 0.20	High
9	0.71	High
10	1.8	Medium
11	0.83	High
12	1.75	Medium
13	2.38	Medium
14	< 0.20	High

*Activity level, high: <0.1 – 1.6, medium: 0.9 – 10.3, and low: 6.3 - >50

For the evaluation of micelle formation, we selected compound **9**, which was predicted most soluble among the fourteen compounds. Protons attached to the methyl and ethyl groups present in its aliphatic side chain (see Fig. S2) were selected to monitor peak broadening since these were easily recognized and differentiated in ^{1}H NMR spectra. Moreover, the aliphatic chain is lipophilic and may contribute to the formation of aggregates of this compound in the buffer solution.

An increasing contribution from peak broadening was observed in ^{1}H-NMR spectra with increasing concentration of **9** from 6.25 µM up to 200 µM (Fig 3A), indicating aggregate formation. The *Mt*SK inhibitory potency of compound **9** was previously determined in our laboratory[20] and reported having the IC$_{50}$ value of 20.73 µM. ^{1}H NMR spectra of compound **9** in Fig. 3A showed peak broadening (aggregation) even at 6.25 µM, which indicates that *Mt*SK inhibition by compound **9** was non-specific, likely due to formation of aggregates. In contrast, riluzole (Fig. S3), a glutamate blocker for treatment of amyotrophic lateral sclerosis[22] and a known non-aggregator,[23] showed no peak broadening across a concentration range from 12.5 – 200 µM (Fig. 3B). Signal intensities displayed sharp resonance and a gradual reduction of signal intensity in alignment with the compound dilution. No signal shifts were observed. Normal NMR resonances should be sharp, and shift in signals should not be expected. There should be no changes in the number and shape of the resonances should be constant.
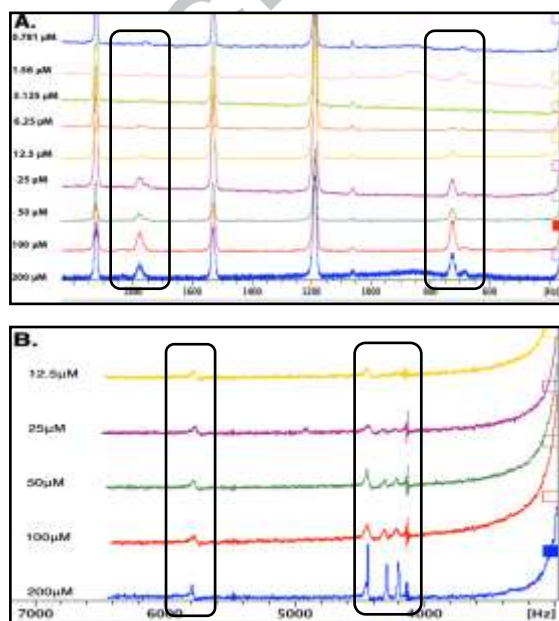

Figure 3. A. ^{1}H NMR spectra of compound **9** producing micelle formation (peak broadening) from 200 µM down to 6.25 µM. Methyl group signal with a chemical shift at 721.6 Hz (Upfield), and ethyl group represent a signal with a chemical shift at 1776.0 Hz (Downfield). B. ^{1}H NMR spectra of a non-aggregator, riluzole (dilutions 200 µM-12.5 µM). Aromatic signals from 4150 Hz to 4490 Hz, no micelle formation, sharp signals as expected, and a gradual decrease of intensity.

We obtained two parameters from our DLS studies, intensity of scattered light and average particle size, both of which increase when aggregation occurs. Compounds **1**-**14** at 100 µM were dissolved in two media, ammonium acetate buffer (Table 8) and water (Table S1). In either solution, scattering intensity and particle size were both large, suggesting aggregation. In comparison, when 0.01% Triton X-100 was also included, light scattering intensity and particle size were both substantially diminished, indicating dissolution of aggregates formed by these compounds. Indeed, in ammonium acetate the average test compound at 100 µM showed a scattering intensity of 292 k count and particle size of 1731 nm in the absence of Triton X-100. Conversely, in the presence of 0.01% Triton X-100, they displayed an average scattering intensity of 136 k count and particle size of 343 nm. Nearly identical results were observed in water (Table S1). These phenomena were in stark contrast with 3-methoxy-4-{[2-({2-methoxy-4-[(4-oxo-2-thioxo-1,3thiazolidin5ylidene)methyl]phenoxy}methyl)benzyl]oxy}ben-zaldehyde, the *Mt*SK-specific control inhibitor, which did not scatter light and did not form particles in either medium until a concentration of 30 µM (three-fold higher than the IC$_{50}$ from Fig. 2). This may be indicative of some aggregation, but even under these conditions both k count and particle size were substantially smaller than the 14 test compounds.

Table 8. Scattering intensities and average particle sizes of test compounds with significant DLS signals in ammonium acetate pH 7.6

Compound Concentration	100 µM			
	Without Triton X-100		With Triton X-100	
Structure	Intensity (Counts)	Size (nm)	Intensity (k Counts)	Size (nm)
1	280	1432	131	255
2	340	2005	158	480
3	310	1820	141	390
4	190	851	83	131
5	240	986	85	151
6	270	1321	115	212
7	350	2850	180	516
8	260	1211	100	201
9	250	1151	100	185
10	300	1620	123	354
11	400	3776	286	817
12	300	1750	139	373
13	321	1934	150	470
14	285	1531	122	271
	Without Triton X-100		With Triton X-100	
Control	Intensity (k Counts)	Size (nm)	Intensity (kCounts)	Size (nm)
30 µM	30	80	5	0
10 µM	4	0	4	0
3 µM	0	0	0	0

To corroborate our DLS investigation, we used transmission electron microscopy (TEM) to image particles formed by each of our 14 candidate compounds in aqueous ammonium acetate. The behavior of compound **14** was typical (Fig. 4A and B). In the absence of Triton X-100, large aggregates were observed (mean size = 0.7µm) (Fig. 4A); however, when Triton X-100 was added, the aggregates were disintegrated, producing particle sizes in the submicron range (Fig. 4B). This confirms the tendency of the compounds toward aggregation and the interference of a detergent like Triton X-100 in that process. At 30 µM, the control exhibited smaller particle size (mean = 0.1µm) (Fig. 4C). Inclusion of Triton X-100 resulted in the dissolution of aggregates, producing a mean size particle of 0.005 µm (Fig. 4D).
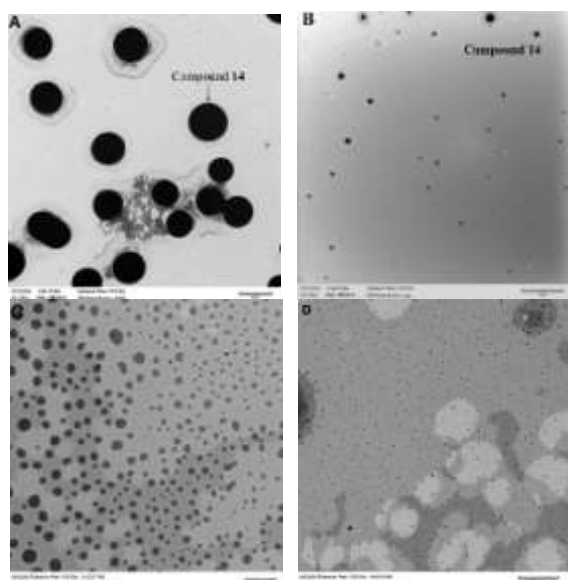
Figure 4. Images visualized by transmission electron microscopy: A. Compound **14** 100 μM formed aggregates with an average size of 0.7 μm (Bar = 1 μm). B. Disrupted aggregates of compound **14** with an average size of 0.03 μm were disrupted by 0.01% v/v Triton X-100 (Bar = 250 nm). C. Control at 30 μM exhibited aggregation with an average size of 100 nm (Bar = 500 nm). D. Control in presence of 0.01% v/v Triton X-100 showed very small particles in the nanometer range with an average size of 5 nm (Bar = 500 nm). All samples were dissolved in ammonium acetate buffer.

When each of the fourteen compounds (50 and 100 μM in buffered solution) was subjected to centrifugation (14,000 × g for 40 min.), pellets were evident by visual inspection (data not shown).

Among the fourteen compounds, **1**, **2**, **3**, **5**, **6**, **7**, **8**, **9**, **10**, and **13** were predicted to form aggregates or micelles, based on the aggregator advisor tool database. Compound **1** had the highest percentage, 93% of similarity to a previously reported aggregator, whereas compounds **8** and **13** had the lomtwest, 72% of similarity within the set. Although compounds **11**, **12**, **14**, and the *Mt*SK-specific inhibitor control did not resemble any previously described aggregator in the aggregator advisor tool database,[24] these were flagged as potential aggregators and suggested for experimental evaluation. Our results clearly show that **14** (Fig. 4) as well as **11** and **12** (Table 8) form aggregates. However, the *Mt*SK-specific control inhibitor showed only a limited capacity to form aggregates (Fig. 4) and (Table 8), and this was at a concentration three-fold greater than the IC_{50}. Aggregation is a likely contributor to inhibition of *Mt*SK by **14** (see Fig. 4). Compound **4** was the only compound from the list that was not flagged. Nevertheless, our approach was able to identify even **4** as an aggregating inhibitor.

An interesting aspect of the fourteen compounds investigated here is that all of them have IC_{90} values < 4 μg/ml in *M. tuberculosis* H37Rv whole-cell screens (Table 7).[17-19] At first glance, this is at variance with the data we present here, showing the strong propensity of all of these compounds to form aggregates and inhibit *Mt*SK on that basis. However, taken together, these data reveal two important conclusions. First, it is likely that complex biological media/intact cells contain certain proteins or other factors that ameliorate aggregate formation or otherwise facilitate compound delivery to the intracellular milieu. This is consistent with what has been noted elsewhere for some known drugs[5] and confirms that a tendency toward aggregation need not be a death sentence for drug development. Second, it

seems clear that the antitubercular properties of these compounds are due to their interaction with a target(s) other than *Mt*SK.

In this study, fourteen compounds, oxadiazole-amides and 2-aminobenzothiazole, have been characterized as non-specific inhibitors of *Mt*SK due to aggregation. This phenomenon was observed across a variety of techniques, including LC-MS, ^{1}H-NMR, DLS, TEM, and centrifugation assays. In general, these assays should serve as practical tools to eliminate false positive hits in early drug discovery process. Detection of promiscuous inhibitors early on saves time and resources. We propose the use of LC-MS and NMR based assays to detect aggregation produced by false positive compounds. These methods are widely used in inhibition studies and routinely available in drug discovery and development laboratories.
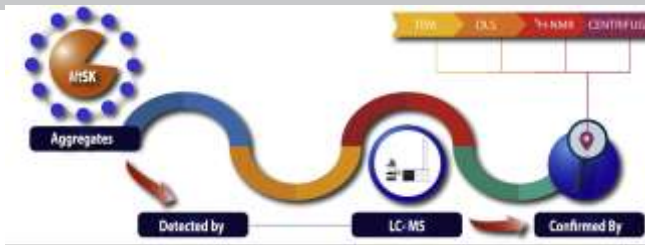
Acknowledgments

Supplementary data

Supplementary data associated with this article can be found, in the online version, at

References

1. Bajorath J. Activity artifacts in drug discovery and different facets of compound promiscuity. *F1000Research*. 2014.

2. Baell JB, Holloway GA. New substructure filters for removal of pan assay interference compounds (PAINS) from screening libraries and for their exclusion in bioassays. *Journal of Medicinal Chemistry*. 2010;53(7):2719-2740.

3. Bruns RF, Watson IA. Rules for identifying potentially reactive or promiscuous compounds. *Journal of Medicinal Chemistry*. 2012;55(22):9763-9772.

4. Shoichet BK. Screening in a spirit haunted world. *Drug Discovery Today*. 2006;11(13-14):607-615.

5. Seidler J, McGovern SL, Doman TN, Shoichet BK. Identification and prediction of promiscuous aggregating inhibitors among known drugs. *Journal of Medicinal Chemistry*. 2003;46(21):4477-4486.

6. Doak AK, Wille H, Prusiner SB, Shoichet BK. Colloid formation by drugs in simulated intestinal fluid. *Journal of Medicinal Chemistry*. 2010;53(10):4259-4265.

7. Giannetti AM, Koch BD, Browner MF. Surface plasmon resonance based assay for the detection and characterization of promiscuous inhibitors. *Journal of Medicinal Chemistry*. 2008;51(3):574-580.

8. Coan KED, Maltby DA, Burlingame AL, Shoichet BK. Promiscuous aggregate-based inhibitors promote enzyme unfolding. *Journal of Medicinal Chemistry*. 2009;52(7):2067-2075.

9. McGovern SL, Shoichet BK. Kinase inhibitors:? not just for kinases anymore. *Journal of Medicinal Chemistry*. 2003;46(8):1478-1483.

10. McGovern SL, Caselli E, Grigorieff N, Shoichet BK. A common mechanism underlying promiscuous inhibitors from virtual and high-throughput screening. *Journal of Medicinal Chemistry*. 2002;45(8):1712-1722.

11. McGovern SL, Helfand BT, Feng B, Shoichet BK. A specific mechanism of nonspecific inhibition. *Journal of Medicinal Chemistry*. 2003;46(20):4265-4272.

12. Hanley RP, Horvath S, An J, Hof F, Wulff JE. Salicylates are interference compounds in TR-FRET assays. *Bioorganic & Medicinal Chemistry Letters*. 2016;26(3):973-977.

13. Coan KED, Shoichet BK. Stoichiometry and physical chemistry of promiscuous aggregate-based inhibitors. *Journal of the American Chemical Society*. 2008;130(29):9606-9612.

14. Baell JB, Ferrins L, Falk H, Nikolakopoulos G. PAINS: Relevance to tool compound discovery and fragment-based screening. *Australian Journal of Chemistry*. 2013;66(12):1483.

15. Coan KED, Shoichet BK. Stability and equilibria of promiscuous aggregates in high protein milieus. *Molecular BioSystems*. 2007;3(3):208.

16. Pohjala L, Tammela P. aggregating behavior of phenolic compounds ? A source of false bioassay results? *Molecules*. 2012;17(12):10774-10790.

17. Reynolds RC, Ananthan S, Faaleolea E, et al. High throughput screening of a library based on kinase inhibitor scaffolds against *Mycobacterium tuberculosis* H37Rv. *Tuberculosis*. 2012;92(1):72-83.

18. Ananthan S, Faaleolea ER, Goldman RC, et al. High-throughput screening for inhibitors of *Mycobacterium tuberculosis* H37Rv. *Tuberculosis*. 2009;89(5):334-353.

19. Maddry JA, Ananthan S, Goldman RC, et al. Antituberculosis activity of the molecular libraries screening center network library. *Tuberculosis*. 2009;89(5):354-363.

20. Simithy J, Reeve N, Hobrath JV, Reynolds RC, Calderon AI. Identification of shikimate kinase inhibitors among anti-*Mycobacterium tuberculosis* compounds by LC-MS. *Tuberculosis*. 2014;94(2):152-158.

21. Merget B, Zilian D, Müller T, Sotriffer CA. MycPermCheck: the *Mycobacterium tuberculosis* permeability prediction tool for small molecules. *Bioinformatics*. 2013;29(1):62-68.

22. Zoccolella S, Beghi E, Palagano G, et al. Riluzole and amyotrophic lateral sclerosis survival: a population-based study in southern Italy: Riluzole and ALS survival in Puglia. *European Journal of Neurology*. 2007;14(3):262-268.

23. LaPlante SR, Carson R, Gillard J, et al. Compound aggregation in drug discovery: implementing a practical NMR assay for medicinal chemists. *Journal of Medicinal Chemistry*. 2013;56(12):5142-5150.

24. Irwin JJ, Duan D, Torosyan H, et al. An aggregation advisor for ligand discovery. *Journal of Medicinal Chemistry*. 2015;58(17):7076-7087.